A Pure Cumulant-Based Method with Low Computational Complexity for Classification and Localization of Multiple Near and Far Field Sources Using a Symmetric Array

Amir Masoud Molaei[1, *], Ali Ramezani Varkani[2], and Mohammad Reza Soheilifar[2]

Abstract—The authors propose a new method based on spatial cumulants for estimating the parameters of multiple near-field and far-field sources. The Toeplitz property used in some studies is not applicable to fourth-order statistics to separate sources components. Therefore, in this paper, a method is proposed to compute output cumulants of specified sensors in special arrangements, by which the components of the near-field and the far-field sources are effectively separated using differencing. The angle and range estimations, as well as the classification of the sources, are obtained based on the data from two spatial cumulant matrices. One of them contains the angle information of all sources, and the other only contains the information of near-field sources. The parameters extraction algorithm is based on the ESPRIT technique; therefore, the proposed method does not require any spectral search. This leads to a significant reduction in computational complexity. Unlike some approaches, the proposed method does not suffer from array aperture loss. Also, the parameters pairing procedure is done automatically. Analysis and simulation results confirm the good performance of the proposed method in terms of computational complexity, estimation accuracy, correct classification of signals, and aperture loss.

1. INTRODUCTION

The direction-of-arrival (DOA) estimation is one of the practical and progressive applications in the field of array signal processing. The main purpose of the DOA estimation is to find the direction of the signals impinging on an antenna array [1]. These signals can be electromagnetic or acoustic waves. The necessity of locating and tracking signal sources in military and civilian applications (such as search and rescue, sonar, seismology, and wireless emergency call locating) shows the importance of DOA estimation. An array can be designed to detect incoming signals so that it only accepts signals from certain directions and rejects ones that are declared as interference.

In many array processing applications, the wave-front is assumed to be planar; in other words, the sources are located in the far-field (FF) of the array. In this case, the task of locating the source is limited to estimating DOAs only. Although plane wave assumption can simplify modeling and processing, such a hypothesis is not valid in practical applications of near-field (NF), as a result, will lead to error in the analysis. When the source is located in the NF or in the Fresnel region of the array aperture, the shape of the spherical wave-front varies nonlinearly with the array position and is characterized by the angle and the range parameters [2]. As a result, the conventional DOA estimation algorithms for far-field sources (FFSs) are not applicable to localization of near-field sources (NFSs). In addition, in some practical applications such as seismic exploration [3], electronic supervision [4], speaker localization

using a microphone array, and guidance system [5, 6], any source can be located in FF or NF. Under such circumstances, conventional methods are encountered with serious drawbacks, since these methods inherently require pure FF or NF signals. Accordingly, in recent years, there has been growing interest in the issue of mixed sources localization.

An efficient method for localization of mixed FFSs and NFSs was first proposed by a two-stage MUSIC algorithm [7], using fourth-order cumulants (FOCs) and spectral search. An algorithm called oblique projection MUSIC was proposed in [8] using second-order statistics (SOS). In [9], an ESPRIT-MUSIC-like method has been developed based on the third-order cyclic moment. Despite the relatively less computational complexity, the reduced range estimation accuracy and some limiting hypotheses are considered as disadvantages in the work [9]. The authors of the study [10] extended the array aperture by using a sparse linear array. Compared to previous algorithms, research [10] has a moderate computational complexity and higher resolution and also has improved the estimation accuracy of parameters. However, it suffers from the problem of spurious peaks concerning range estimation. A method based on constructing spatial-temporal cumulants is presented in [11], which does not need to know the number of sources. Based on the generalized ESPRIT (GESPRIT) algorithm [12], several methods have been proposed to localize mixed sources [6, 13–15]. Compared to other SOS-based methods, the algorithm [13] has improved the estimation accuracy and also made a more reasonable classification of signals types. The covariance differencing method presented in [14, 15] provides a reasonable classification. For GESPRIT-based algorithms, the maximum number of resolvable NFSs is less than half of the array's sensors [16]. In [17], an SOS-based method is proposed to estimate the DOA, range, and frequency parameters, which avoids multi-dimensional spectral search. The use of the mixed second and fourth order statistics with applying the MUSIC technique is considered in research [18], which provides a reasonable classification. However, it sets strict limits on the DOA intervals of incoming signals. In the study [19], a mixed order statistics method based on cumulant matrix reconstruction and the use of MUSIC spectrum has been presented, which provides good accuracy.

All of the above methods require heavy computations of spectral search. In addition, the methods [7, 11, 18, 19] have a higher computational burden due to the construction of fourth-order statistics (FOS) matrices along with spectral search. On the other hand, the aperture loss that appears in works [6, 8, 9, 14, 15, 19] is another issue that should be considered about the number of sensors. Also, in the case of NFSs, in addition to the DOA and range estimations, the pairing between these two parameters should also be made. The differencing operation presented in [14, 15] is valid only for SOS, and according to what we will show in the text, for FOS-based methods, the Toeplitz property will no longer help to separate the FF and NF components.

What will be presented in this paper is an algorithm that, in addition to efficient separation of the FF and NF components in the cumulant domain, estimates the parameters of the mixed NFSs and FFSs without the need for a pairing process and with the lowest aperture loss. The use of high-order statistics, in addition to increasing the estimation accuracy, also allows saving the number of sensors [20]. In addition, FOCs are not sensitive to any kind of Gaussian noise. In the proposed method, the signals are received by a symmetric uniform linear array (ULA). Five special cumulants are defined, and five corresponding matrices are constructed based on the received data. The first matrix only contains the angle information, and the sources' DOAs are extracted from it. Four other matrices, pairwise, contain common FF information. By two differencing operations, FFSs information is eliminated. The information needed to classify sources and estimate the NFSs parameters is obtained by providing an ESPRIT-based method.

The rest of this paper is organized as follows. In Section 2, the mathematical model of the data and main assumptions are expressed. In Section 3, the proposed algorithm is completely explained. Section 4 deals with the performance analysis of the proposed algorithm. Simulations and their results are presented in Section 5. Conclusions are given in Section 6. Also, details of some equations and proofs are given in the Appendix.

Notation: Throughout the paper, superscripts T, H, and $*$ represent the transpose, conjugate transpose, and complex conjugate, respectively. Symbols $\hat{x}$, $E\{x\}$, and $\lfloor x \rfloor$ stand for the estimation, mathematical expectation, and floor of x, respectively. $\mathbf{J}_{x \times y}$ represents the matrix of ones of size $x \times y$. j is the imaginary unit.

2. DATA MODEL

Consider N uncorrelated narrowband sources including N_N NFSs and N_F FFSs. The signals transmitted by these sources impinge on a symmetric ULA consisting of $2M + 1$ sensors with element spacing d from the directions $\theta_1, \theta_2, \ldots, \theta_N$ (Fig. 1). Each element is denoted by an index l, where $l = -M, \ldots, 0, \ldots, M$. The array steering vector for the ith incoming signal and the lth sensor is defined by

$$a_{li} = e^{jT_{li}} \tag{1}$$

where T_{li} refers to the phase shift related to the ith signal due to the propagation time delay between the reference sensor and the lth sensor, and $i = 1, 2, \ldots, N$. Considering the array center as the phase reference, if the ith source is located in the NF, then T_{li} can be approximated as [7, 15, 21]

$$T_{li} \approx \gamma_i l + \phi_i l^2 \tag{2}$$

where the electric angles γ_i and ϕ_i are derived as follows:

$$\gamma_i = -2\pi \frac{d}{\lambda} \sin \theta_i, \quad \phi_i = \pi \frac{d^2}{\lambda r_i} \cos^2 \theta_i \tag{3}$$

where λ is the wavelength, and r_i is the range of the ith source. On the other hand, if the ith source is located in the FF $(r_i \to \infty)$, then T_{li} can be considered as [7, 15]

$$T_{li} \approx \gamma_i l. \tag{4}$$
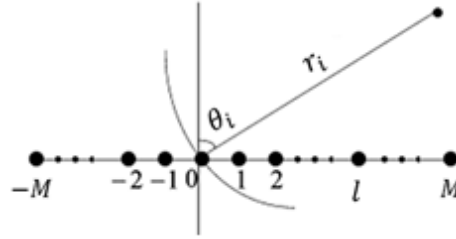
Figure 1. A symmetric ULA consisting of $2M + 1$ sensors.

With a proper sampling rate, the kth sample of the signal observed by the lth sensor is expressed as [22]

$$x_l(k) = \sum_{i=1}^{N} s_i(k) e^{jT_{li}} + n_l(k), \quad k = 1, \ldots, N_s \tag{5}$$

where N_s, $s_i(t)$, and $n_l(t)$ are the number of snapshots, signal of the ith source, and noise of the lth sensor, respectively. Without the loss of generality, we assume that the first N_N signals are received from the NF and the remaining signals from the FF, so Eq. (5) can be rewritten as

$$x_l(k) = \sum_{i=1}^{N_N} s_i(k) e^{j(\gamma_i l + \phi_i l^2)} + \sum_{i=N_N+1}^{N} s_i(k) e^{j\gamma_i l} + n_l(k). \tag{6}$$

In matrix form, the array output vector is expressed as

$$\mathbf{x}(k) = \mathbf{A}\mathbf{s}(k) + \mathbf{n}(k) \tag{7}$$

whose vectors and matrices are determined by

$$\mathbf{x}(t) = [x_{-M}(t) \ \ldots \ x_0(t) \ \ldots \ x_M(t)]^T$$
$$\mathbf{s}(t) = [\mathbf{s}_N^T(t) \ \mathbf{s}_F^T(t)]^T$$
$$\mathbf{s}_N(t) = [s_1(t) \ s_2(t) \ \ldots \ s_{N_N}(t)]^T \tag{8}$$
$$\mathbf{s}_F(t) = [s_{N_N+1}(t) \ s_{N_N+2}(t) \ \ldots \ s_N(t)]^T$$
$$\mathbf{n}(t) = [n_{-M}(t) \ \ldots \ n_0(t) \ \ldots \ n_M(t)]^T$$

where $\mathbf{s}_N(t) \in \mathbb{C}^{N_N \times 1}$, $\mathbf{s}_F(t) \in \mathbb{C}^{N_F \times 1}$ and $\mathbf{n}(t) \in \mathbb{C}^{(2M+1) \times 1}$ are the source vector of the NF and FF signals, and the additive Gaussian noise vector with mean zero. $\mathbf{A} \in \mathbb{C}^{(2M+1) \times N}$ is the steering matrix and can be written as

$$\mathbf{A} = [\mathbf{A}_N \ \mathbf{A}_F], \quad \mathbf{A}_N = [\mathbf{a}_1 \ \mathbf{a}_2 \ \ldots \ \mathbf{a}_{N_N}]$$
$$\mathbf{A}_F = [\mathbf{a}_{N_N+1} \ \ldots \ \mathbf{a}_N], \quad \mathbf{a}_i = [a_{-Mi} \ a_{-M+1i} \ \ldots \ a_{Mi}]^T \tag{9}$$

where a_{li} can be determined by Eqs. (1), (2), and (4).

The following basic hypotheses are assumed to hold:

1- The array is calibrated, and the matrix $\mathbf{A}$ is full rank.

2- The signals $\{\mathbf{s}_i(t)\}_{i=1}^N$ are statistically mutually independent, narrowband stationary processes with nonzero kurtosis.

3- Sensor noise is the additive (white or color) Gaussian one and statistically independent of sources signals.

4- The sensor array is a ULA arranged by element spacing $d \leq \lambda/4$, in order to avoid the phase ambiguity [23].

5- The number of elements satisfies both $2M + 1 > N$ and $2M + 1 \geq N_N + 2$.

6- Signals' DOAs are different.

3. PROPOSED METHOD

In this section, first, some special cumulant matrices are defined. The proposed method is then fully explained.

3.1. Definition and Construction of Special Cumulant Matrices

Since the proposed method uses FOS, we consider five cross-cumulant functions $c_{4x,1}(\bar{u}, \bar{v})$, $c_{4x,2}(u, v)$, $c_{4x,3}(u, v)$, $c_{4x,4}(u, v)$ and $c_{4x,5}(u, v)$ for the array output stationary signals with a common zero time lag and different sensor lags in the following form:

$$c_{4x,1}(\bar{u}, \bar{v}) = Cum\left\{x_{\bar{u}}^*(k), x_{\bar{v}}(k), x_{-\bar{v}}^*(k), x_{-\bar{u}}(k)\right\}$$
$$c_{4x,2}(u, v) = Cum\left\{x_u^*(k), x_{u+1}(k), x_{v+1}^*(k), x_v(k)\right\}$$
$$c_{4x,3}(u, v) = Cum\left\{x_u^*(k), x_{u+1}(k), x_v^*(k), x_{v-1}(k)\right\} \tag{10}$$
$$c_{4x,4}(u, v) = Cum\left\{x_{u-1}^*(k), x_u(k), x_{-v}^*(k), x_{1-v}(k)\right\}$$
$$c_{4x,5}(u, v) = Cum\left\{x_u^*(k), x_{u+1}(k), x_{-v}^*(k), x_{1-v}(k)\right\}$$

where $\bar{u}, \bar{v} \in [-M, M]$ and $u, v \in [-M+1, M-1]$. According to assumptions 2 and 3, the result of the cumulants of Eq. (10) can be written as (see Appendix A for more details)

$$c_{4x,1}(\bar{u}, \bar{v}) = \sum_{i=1}^{N} c_{s_i} e^{-j2\bar{u}\gamma_i} e^{j2\bar{v}\gamma_i}$$

$$c_{4x,2}(u, v) = \sum_{i=1}^{N_N} c_{s_i} e^{j2u\phi_i} e^{-j2v\phi_i} + \sum_{i=N_N+1}^{N} c_{s_i}$$

$$c_{4x,3}(u, v) = \sum_{i=1}^{N_N} c_{s_i} e^{j2(u+1)\phi_i} e^{-j2v\phi_i} + \sum_{i=N_N+1}^{N} c_{s_i} \tag{11}$$

$$c_{4x,4}(u, v) = \sum_{i=1}^{N_N} c_{s_i} e^{j2u\phi_i} e^{-j2v\phi_i} e^{j2\gamma_i} + \sum_{i=N_N+1}^{N} c_{s_i} e^{j2\gamma_i}$$

$$c_{4x,5}(u, v) = \sum_{i=1}^{N_N} c_{s_i} e^{j2(u+1)\phi_i} e^{-j2v\phi_i} e^{j2\gamma_i} + \sum_{i=N_N+1}^{N} c_{s_i} e^{j2\gamma_i}$$

where $c_{s_i} = Cum\{s_i^*(t), s_i(t), s_i^*(t), s_i(t)\}$ is the kurtosis related to the ith signal. According to Eq. (11) and by collecting all sensor lags, we can construct the complex cross-cumulant matrices of the sensors in the following form:

$$\mathbf{C}_1 = \mathbf{B}\mathbf{C}_s\mathbf{B}^H, \quad \mathbf{C}_2 = \mathbf{D}\mathbf{C}_s\mathbf{D}^H, \quad \mathbf{C}_3 = \mathbf{D}\mathbf{\Phi}\mathbf{C}_s\mathbf{D}^H$$
$$\mathbf{C}_4 = \mathbf{D}\mathbf{\Upsilon}\mathbf{C}_s\mathbf{D}^H, \quad \mathbf{C}_5 = \mathbf{D}\mathbf{\Phi}\mathbf{\Upsilon}\mathbf{C}_s\mathbf{D}^H. \tag{12}$$

Equation (13) gives the value of the $(\widehat{u}, \widehat{v})$th element of matrix $\mathbf{C}_1$ according to the definitions $\widehat{u} = \bar{u} + M + 1$ and $\widehat{v} = \bar{v} + M + 1$. Also, by defining $\tilde{u} = u + M$ and $\tilde{v} = v + M$, the $(\tilde{u}, \tilde{v})$th element of matrices $\mathbf{C}_2$, $\mathbf{C}_3$, $\mathbf{C}_4$, and $\mathbf{C}_5$ can be obtained from Eq. (13) (see Appendix A for their practical estimation)

$$\mathbf{C}_1(\widehat{u}, \widehat{v}) = Cum\left\{x_{\widehat{u}}^*(t), x_{\widehat{v}}(t), x_{N-\widehat{v}+1}^*(t), x_{N-\widehat{u}+1}(t)\right\}$$
$$\mathbf{C}_2(\tilde{u}, \tilde{v}) = Cum\left\{x_{\tilde{u}+1}^*(t), x_{\tilde{u}+2}(t), x_{\tilde{v}+2}^*(t), x_{\tilde{v}+1}(t)\right\}$$
$$\mathbf{C}_3(\tilde{u}, \tilde{v}) = Cum\left\{x_{\tilde{u}+1}^*(t), x_{\tilde{u}+2}(t), x_{\tilde{v}+1}^*(t), x_{\tilde{v}}(t)\right\} \tag{13}$$
$$\mathbf{C}_4(\tilde{u}, \tilde{v}) = Cum\left\{x_{\tilde{u}}^*(t), x_{\tilde{u}+1}(t), x_{M-\tilde{v}}^*(t), x_{M+1-\tilde{v}}(t)\right\}$$
$$\mathbf{C}_5(\tilde{u}, \tilde{v}) = Cum\left\{x_{\tilde{u}+1}^*(t), x_{\tilde{u}+2}(t), x_{M-\tilde{v}}^*(t), x_{M+1-\tilde{v}}(t)\right\}$$

where $\widehat{u}, \widehat{v} \in [1, 2M + 1]$ and $\tilde{u}, \tilde{v} \in [1, 2M - 1]$. Therefore, the first matrix of Eq. (12) is of size $(2M + 1) \times (2M + 1)$, and the last four matrices are of size $(2M - 1) \times (2M - 1)$. $\mathbf{C}_s \in \mathbb{R}^{N \times N}$, $\mathbf{\Upsilon} \in \mathbb{C}^{N \times N}$ and $\mathbf{\Phi} \in \mathbb{C}^{N \times N}$ are the diagonal matrices defined in the following form:

$$\mathbf{\Phi} = \text{diag}\left[e^{j2\phi_1}, e^{j2\phi_2}, \ldots, e^{j2\phi_{N_N}}, 1, \ldots, 1\right]$$
$$\mathbf{\Upsilon} = \text{diag}\left[e^{j2\gamma_1}, e^{j2\gamma_2}, \ldots, e^{j2\gamma_N}\right] \tag{14}$$
$$\mathbf{C}_s = \text{diag}\left[c_{s_1}, c_{s_2}, \ldots, c_{s_N}\right].$$

In this way, $\mathbf{B} \in \mathbb{C}^{(2M-1) \times N}$ is obtained by

$$\mathbf{B} = \begin{bmatrix} e^{j2(2M)\gamma_1} & e^{j2(2M)\gamma_2} & \cdots & e^{j2(2M)\gamma_N} \\ e^{j2(2M-1)\gamma_1} & e^{j2(2M-1)\gamma_2} & \cdots & e^{j2(2M-1)\gamma_N} \\ \vdots & \vdots & \ddots & \vdots \\ 1 & 1 & \cdots & 1 \end{bmatrix}. \tag{15}$$

Also, matrix $\mathbf{D} \in \mathbb{C}^{(2M-1) \times N}$ is of rank $N_N + 1$ (according to assumption 6), in which the elements of the last N_F columns are equal to 1, and the elements of the first N_N columns contain information about ϕ_i. $\mathbf{D}$ is obtained by

$$\mathbf{D} = \begin{bmatrix} \mathbf{D}_N & \mathbf{J}_{(2M-1) \times N_F} \end{bmatrix}$$
$$\mathbf{D}_N = \begin{bmatrix} 1 & \cdots & 1 \\ e^{j2\phi_1} & \cdots & e^{j2\phi_{N_N}} \\ \vdots & \ddots & \vdots \\ e^{j2(2M-2)\phi_1} & \cdots & e^{j2(2M-2)\phi_{N_N}} \end{bmatrix}. \tag{16}$$

3.2. Sources' DOA Estimation

In the proposed method, the information of the last four matrices of Eq. (12) alone is not sufficient to find the DOA of the FFSs and to classify the signals types. The first matrix only contains the DOA information, which we only use in this section.

We form two overlapping matrices $\mathbf{C}_{11} \in \mathbb{C}^{2M \times (2M+1)}$ and $\mathbf{C}_{12} \in \mathbb{C}^{2M \times (2M+1)}$ as

$$\mathbf{C}_{11} = \mathbf{B}_1\mathbf{C}_s\mathbf{B}^H, \quad \mathbf{C}_{12} = \mathbf{B}_2\mathbf{C}_s\mathbf{B}^H \tag{17}$$

where $\mathbf{C}_{11}$ and $\mathbf{C}_{12}$ consist of the first $2M$ and the last $2M$ rows of the Hermitian matrix $\mathbf{C}_1$, respectively. $\mathbf{B}_1 \in \mathbb{C}^{2M \times N}$ and $\mathbf{B}_2 \in \mathbb{C}^{2M \times N}$, respectively, include the first $2M$ and the last $2M$ rows of $\mathbf{B}$, and they hold the following equation:

$$\mathbf{B}_2 = \mathbf{B}_1 \boldsymbol{\psi} \tag{18}$$

where $\boldsymbol{\psi} = \mathrm{diag}[e^{-j2\gamma_1}, \ldots, e^{-j2\gamma_N}]$ contains the angle information of all sources. According to assumptions 5 and 6, $\mathbf{B}_1$ and $\mathbf{B}^H$ are full column and full row rank, respectively. We form the *angle estimation matrix* as

$$\mathbf{C}_A = \left(\mathbf{C}_{11}^H \mathbf{C}_{11}\right)^{-1} \mathbf{C}_{11}^H \mathbf{C}_{12} = \left(\mathbf{B}^H \mathbf{B}\right)^{-1} \mathbf{B}^H \boldsymbol{\psi} \mathbf{B}. \tag{19}$$

By applying the eigenvalue decomposition (EVD) to $\mathbf{C}_A$, we have

$$\mathbf{C}_A = \mathbf{U} \boldsymbol{\Sigma} \mathbf{U}^{-1} \tag{20}$$

where $\boldsymbol{\Sigma} = \mathrm{diag}[\sigma_1, \ldots, \sigma_{2M+1}]$ is a diagonal matrix with the eigenvalues arranged as $|\sigma_1| \geq \ldots \geq |\sigma_N| > |\sigma_{N+1}| > \ldots > |\sigma_{2M+1}|$. A part of $\mathbf{U} \in \mathbb{C}^{(2M+1) \times (2M+1)}$ contains N eigenvectors related to eigenvalues $\sigma_1, \ldots, \sigma_N$, which spans the signal subspace of $\mathbf{C}_A$.

The sources' DOAs can easily extract from Eq. (21)

$$\hat{\theta}_i = \arcsin\left(\frac{\lambda \angle \sigma_i}{4\pi d}\right), \quad i = 1, \ldots, N \tag{21}$$

where $\sigma_i = e^{-j2\hat{\gamma}_i}$. We define the angles estimation vector as $\hat{\theta} = [\hat{\theta}_1, \ldots, \hat{\theta}_N]$. Equation (21) alone cannot determine which DOAs belong to NFSs and which belong to the FFSs.

3.3. NF and FF Components Separation by Differencing in the Cumulant Domain

In this section, a new method is proposed for separating the components of the NF and the FF in the cumulant domain. With respect to Eq. (13), each of the last four matrices in Eq. (12) can be written as the sum of two cumulant matrices, one containing only the information of the NF components, and the other one only contains FF information, namely

$$\begin{aligned}
\mathbf{C}_2 &= \mathbf{C}_{N1} + \mathbf{C}_{F1}, \quad \mathbf{C}_3 = \mathbf{C}_{N2} + \mathbf{C}_{F1} \\
\mathbf{C}_4 &= \mathbf{C}_{N3} + \mathbf{C}_{F2}, \quad \mathbf{C}_5 = \mathbf{C}_{N4} + \mathbf{C}_{F2}.
\end{aligned} \tag{22}$$

According to Appendix B, both NF and FF parts of the above matrices are Toeplitz. Therefore, the use of algorithms such as [14, 15], which take advantage of being Toeplitz of the FF covariance matrix and being non-Toeplitz of the NF covariance matrix for the separation of components, cannot be implemented here for FOS.

Now, by simple differencing between the pair of matrices $\mathbf{C}_2$, $\mathbf{C}_3$ and $\mathbf{C}_4$, $\mathbf{C}_5$, we have

$$\begin{aligned}
\mathbf{C}_{32} &= \mathbf{C}_3 - \mathbf{C}_2 = \mathbf{C}_{N2} - \mathbf{C}_{N1} \\
\mathbf{C}_{54} &= \mathbf{C}_5 - \mathbf{C}_4 = \mathbf{C}_{N4} - \mathbf{C}_{N3}.
\end{aligned} \tag{23}$$

The matrices $\mathbf{C}_{32} \in \mathbb{C}^{(2M-1) \times (2M-1)}$ and $\mathbf{C}_{54} \in \mathbb{C}^{(2M-1) \times (2M-1)}$ only contain the information of the NF components and are given in Eq. (24).

$$\mathbf{C}_{32} = j2 \cdot \begin{bmatrix}
\begin{matrix} c_{s_1} e^{j\phi_1} \sin\phi_1 + \ldots \\ + c_{s_{N_N}} e^{j\phi_{N_N}} \sin\phi_{N_N} \end{matrix} & \cdots & \begin{matrix} c_{s_1} e^{-j(4M-5)\phi_1} \sin\phi_1 + \ldots \\ + c_{s_{N_N}} e^{-j(4M-5)\phi_{N_N}} e^{j\phi_{N_N}} \sin\phi_{N_N} \end{matrix} \\
\begin{matrix} c_{s_1} e^{j3\phi_1} \sin\phi_1 + \ldots \\ + c_{s_{N_N}} e^{j3\phi_{N_N}} \sin\phi_{N_N} \end{matrix} & \cdots & \begin{matrix} c_{s_1} e^{-j(4M-7)\phi_1} \sin\phi_1 + \ldots \\ + c_{s_{K_N}} e^{-j(4M-7)\phi_{N_N}} \sin\phi_{N_N} \end{matrix} \\
\vdots & \ddots & \vdots \\
\begin{matrix} c_{s_1} e^{j(4M-3)\phi_1} \sin\phi_1 + \ldots \\ + c_{s_{N_N}} e^{j(4M-3)\phi_{N_N}} \sin\phi_{N_N} \end{matrix} & \cdots & \begin{matrix} c_{s_1} e^{j\phi_1} \sin\phi_1 + \ldots \\ + c_{s_{N_N}} e^{j\phi_{N_N}} \sin\phi_{N_N} \end{matrix}
\end{bmatrix}$$

$$
\mathbf{C}_{54} = j2 \cdot
\begin{bmatrix}
c_{s_1} e^{j\phi_1} e^{j2\gamma_1} \sin\phi_1 + \dots & & c_{s_1} e^{-j(4M-5)\phi_1} e^{j2\gamma_1} \sin\phi_1 + \dots \\
+ c_{s_{K_N}} e^{j\phi_{N_N}} e^{j2\gamma_{N_N}} \sin\phi_{N_N} & \cdots & + c_{s_{N_N}} e^{-j(4M-5)\phi_{N_N}} e^{j\gamma_{N_N}} \sin\phi_{N_N} \\
c_{s_1} e^{j3\phi_1} e^{j2\gamma_1} \sin\phi_1 + \dots & & c_{s_1} e^{-j(4M-7)\phi_1} e^{j2\gamma_1} \sin\phi_1 + \dots \\
+ c_{s_{N_N}} e^{j3\phi_{N_N}} e^{j2\gamma_{N_N}} \sin\phi_{N_N} & \cdots & + c_{s_{K_N}} e^{-j(4M-7)\phi_{N_N}} e^{j\gamma_{N_N}} \sin\phi_{N_N} \\
\vdots & \ddots & \vdots \\
c_{s_1} e^{j2(2M-1)\phi_1} e^{j2\gamma_1} \sin\phi_1 + \dots & & c_{s_1} e^{j2\phi_1} e^{j2\gamma_1} \sin\phi_1 + \dots \\
+ c_{s_{K_N}} e^{j2(2M-1)\phi_{N_N}} e^{j2\gamma_{N_N}} \sin\phi_{N_N} & \cdots & + c_{s_{N_N}} e^{j2\phi_{N_N}} e^{j\gamma_{N_N}} \sin\phi_{N_N}
\end{bmatrix}
\tag{24}
$$

In this way, we are able to separate the pure NF components from the entire data in the cumulant domain. In the next section, we will use this information to estimate the range and DOA of NFSs.

3.4. NFSs DOA Identification and Range Estimation

In the previous section, we showed how we can obtain pure NF information from the observed data using the cumulant differencing. The difference matrices $\mathbf{C}_{32}$ and $\mathbf{C}_{54}$ can be decomposed as the multiplication of matrices $\mathbf{D}_N$, $\mathbf{C}_{sN}$, $\mathbf{\Phi}_N$, and $\mathbf{\Upsilon}_N$ as

$$
\mathbf{C}_{32} = \mathbf{D}_N \mathbf{\Phi}_N \mathbf{C}_{sN} \mathbf{D}_N^H, \quad \mathbf{C}_{54} = \mathbf{D}_N \mathbf{\Phi}_N \mathbf{\Upsilon}_N \mathbf{C}_{sN} \mathbf{D}_N^H
\tag{25}
$$

where $\mathbf{C}_{sN}$, $\mathbf{\Phi}_N$, $\mathbf{\Upsilon}_N \in \mathbb{C}^{N_N \times N_N}$ are derived from Eq. (26)

$$
\begin{aligned}
\mathbf{C}_{sN} &= \operatorname{diag}\left[c_{s_1}, c_{s_2}, \dots, c_{s_{N_N}} \right] \\
\mathbf{\Phi}_N &= j2 \cdot \operatorname{diag}\left[e^{j\phi_1} \sin\phi_1, e^{j\phi_2} \sin\phi_2, \dots, e^{j\phi_{N_N}} \sin\phi_{N_N} \right] \\
\mathbf{\Upsilon}_N &= \operatorname{diag}\left[e^{j2\gamma_1}, e^{j2\gamma_2}, \dots, e^{j2\gamma_{N_N}} \right].
\end{aligned}
\tag{26}
$$

Given assumptions 1 and 6, in order for $\mathbf{D}_N$ to be a full column rank matrix, it is necessary and sufficient that the number of sensors satisfies $2M + 1 \geq N_N + 2$; this condition corresponds to assumption 5.

The two equations expressed in Eq. (25) can be considered as the basic equations of ESPRIT [24]. Therefore, we define the NF parameters estimation matrix $\mathbf{C}_N \in \mathbb{C}^{(2M-1) \times (2M-1)}$ as

$$
\mathbf{C}_N = \mathbf{C}_{32} \left(\mathbf{C}_{54}^H \mathbf{C}_{54} \right)^{-1} \mathbf{C}_{54}^H.
\tag{27}
$$

According to assumption 5, $\mathbf{D}_N$ is full column rank, and it can easily be shown that $\mathbf{D}_N^H \in \mathbb{C}^{N_N \times (2M-1)}$ is a full row rank matrix [25]. On the other hand, according to assumption 2, $\mathbf{C}_{sN}$ has no zero singular value, and there are no two identical elements on the main diagonal of $\mathbf{\Phi}_N$ and $\mathbf{\Upsilon}_N$ (except for $\theta = \pm 90°$). Therefore, we can rewrite Eq. (27) as

$$
\mathbf{C}_N = \mathbf{D}_N \mathbf{\Upsilon}_N^{-1} \left(\mathbf{D}_N^H \mathbf{D}_N \right)^{-1} \mathbf{D}_N^H
\tag{28}
$$

where $\mathbf{B}_N^{H\dagger}$ is full column rank.

Given that $\mathbf{D}_N$ is full column rank, to estimate the electric angles of the NFSs, we need to apply EVD to $\mathbf{C}_N$

$$
\mathbf{C}_N = \mathbf{Q}\mathbf{\Lambda}\mathbf{Q}^{-1} = [\mathbf{q}_1, \dots, \mathbf{q}_{2M-1}] \operatorname{diag}[\mu_1, \dots, \mu_{2M-1}][\mathbf{q}_1, \dots, \mathbf{q}_{2M-1}]^{-1}
\tag{29}
$$

where $\mathbf{\Lambda} \in \mathbb{C}^{(2M-1) \times (2M-1)}$ is a diagonal matrix with eigenvalues arranged as $\mu_1 \geq \dots \geq \mu_N > \mu_{N+1} = \dots = \mu_{2M-1} = 0$, and $\mathbf{Q} \in \mathbb{C}^{(2M-1) \times (2M-1)}$ is the matrix of eigenvectors with column vectors $\mathbf{q}_{i'}$ ($i' = 1, \dots, 2M-1$). N_N non-zero eigenvalues (from N non-zero eigenvalues) obtained from the EVD of $\mathbf{C}_N$ give an estimate of the diagonal elements of the matrix $\mathbf{\Upsilon}_N^{-1}$ (that is $e^{-j2\hat{\gamma}_i}$, $i = 1, \dots, N_N$) containing the information of the NFSs' DOA. Therefore, we can choose the NFSs' DOAs from the values estimated by Eq. (30)

$$
\hat{\vartheta}_i = \arcsin\left(\frac{\lambda \angle \mu_i}{4\pi d} \right), \quad i = 1, 2, \dots, N
\tag{30}
$$

N_N common values between the $\hat{\vartheta}_i$s in Eq. (30) and the angles estimated in $\hat{\theta}$ are considered as valid DOAs of the NFSs, which form the vector $\hat{\theta}_N \in \mathbb{R}^{1 \times K_N}$. The rest of the elements of vector $\hat{\theta}$ are considered as DOAs of the FFSs.

On the other hand, the N_N eigenvectors $\mathbf{q}_{i'}$ ($i' = 1, \ldots, N_N$), corresponding to the valid $\hat{\vartheta}_i$s, can give an estimate of $\mathbf{D}_N$. By dividing the elements of the $m + 1$th row of $\mathbf{q}_{i'}$ by the corresponding elements of the mth row ($m = 1, \ldots, 2M - 3$), we can extract an estimate of $\phi_{i'}$ as

$$\hat{\phi}_{i'} = \frac{1}{2} \measuredangle \frac{1}{2M - 3} \sum_{m=1}^{2M-3} \frac{q_{m+1, i'}}{q_{m, i'}}, \quad i' = 1, \ldots, N_N \tag{31}$$

where $q_{m, i'}$ is the element of the mth row of $\mathbf{q}_{i'}$. Given Eqs. (3) and (31), we can calculate the NFSs' range by

$$\hat{r}_{i'} = \frac{\pi d^2 \cos\left(\hat{\theta}_{i'}\right)}{\lambda \hat{\phi}_{i'}}, \quad i' = 1, \ldots, N_N \tag{32}$$

where $\hat{\theta}_i$ is the mth member of $\hat{\theta}_N$.

4. ANALYSIS AND DISCUSSION

In this section, we analyze and discuss the proposed algorithm from four ways including computational complexity, aperture loss, parameters pairing, and NFS localization at the same angle with the FFS.

4.1. Computational Complexity

Here, we compare computational complexity [26] of the proposed method, considering the major multiplications.

The method [7] requires constructing two fourth-order matrices with dimensions $(2M + 1) \times (2M + 1)$ and $(4M + 1) \times (4M + 1)$, applying EVD to them, and performing the one-dimensional MUSIC spectral search for direction estimation. In addition, the range estimation requires N times the EVD implementation on matrices of size $(8M + 5) \times (8M + 5)$. Therefore, the number of operations required in the work [7] is equal to

$$9 \left(2M + 1\right)^2 N_s + 9 \left(4M + 1\right)^2 N_s + \frac{4}{3} \left(2M + 1\right)^3 + \frac{4}{3} \left(4M + 1\right)^3 + \frac{4}{3} N \left(8M + 5\right)^3 + \frac{180}{\Delta_\theta} \left(2M + 1\right)^2 \tag{33}$$

where Δ_θ is the angle search step in degree.

The method [8] involves the construction of one covariance matrix of size $(2M + 1) \times (2M + 1)$ and another covariance matrix of size $(M + 2) \times (M + 2)$ (by selecting $\lfloor \frac{M+1}{2} \rfloor$ as the number of overlapping subvectors), applying EVD to them, spectral search implementation for the DOA estimation, and N times the spectral search implementation for range. Therefore, the number of operations required in [8] is equal to

$$(2M + 1)^2 N_s + (M + 2)^2 N_s + \frac{4}{3} \left(2M + 1\right)^3 + \frac{1}{3} \left(M + 2\right)^3$$

$$+ \frac{180}{\Delta_\theta} \left(2M + 1\right)^2 + N \frac{2D^2/\lambda - 0.62\sqrt{D^3/\lambda}}{\Delta_r} \left(2M + 1\right)^2 \tag{34}$$

where Δ_r is the range search step in terms of wavelength.

The method [15] constructs one $(2M + 1) \times (2M + 1)$ covariance matrix, computes its SVD, along with the SVD of the covariance difference matrix (with dimension $(2M + 1) \times (2M + 1)$) and the FF matrix (with dimension $(2M + 1) \times (2M + 1)$). In addition, two spectral searches for the angle and N_N times spectral search for the range are required. Therefore, the sum of multiplications in [15] is equal to

$$(2M + 1)^2 N_s + 4 \left(2M + 1\right)^3 + \frac{720}{\Delta_\theta} M^2 + \frac{180}{\Delta_\theta} \left(2M + 1\right)^2 + N_N \frac{2D^2/\lambda - 0.62\sqrt{D^3/\lambda}}{\Delta_r} \left(2M + 1\right)^2. \tag{35}$$

The method [11] constructs L cumulant matrices and one covariance matrix with dimensions $(2M+1) \times (2M+1)$. Also, it constructs two other matrices, one with dimension $(2M+1) \times (2M+1)$ (requiring the product of L cumulant matrices with their Hermitian) and the other one with dimension $(2M+1) \times L$ (requiring the product of L cumulant matrices with the virtual steering vector). It also requires an EVD (on a $L \times L$ matrix) in the process of finding the DOA and an EVD on the covariance matrix. In addition, spectral searches for finding direction and range are also a part of its implementation process. Therefore, the number of operations required in [11] is equal to

$$(9L+1)(2M+1)^2 N_s + 2L(2M+1)^2(M+1) + \frac{4}{3}(2M+1)^3 + \frac{4}{3}L^3$$

$$+\frac{180}{\Delta_\theta}(2M+1)^2 + N\frac{2D^2/\lambda - 0.62\sqrt{D^3/\lambda}}{\Delta_r}(2M+1)^2. \tag{36}$$

The method [18] constructs one $(2M+1) \times (2M+1)$ covariance matrix and one cumulant matrix of the same size. Also, it constructs one FF cumulant matrix. Furthermore, it requires an EVD on the covariance matrix and an EVD on the NF cumulant matrix. In addition, spectral searches for finding the direction of both NFSs and FFSs, and range estimation are also a part of its implementation process. Therefore, the number of operations required in [18] is equal to

$$10(2M+1)^2 N_s + N(2M+1)^2 + \frac{8}{3}(2M+1)^3$$

$$+\frac{360}{\Delta_\theta}(2M+1)^2 + N_N\frac{2D^2/\lambda - 0.62\sqrt{D^3/\lambda}}{\Delta_r}(2M+1)^2. \tag{37}$$

The method [19] constructs one $(2M+1) \times (2M+1)$ covariance matrix and one cumulant matrix of the same size. It also implements their EVD and performs EVD on the NF cumulant matrix. In addition, spectral searches for finding both direction and range are also a part of its implementation process. Therefore, the number of operations required in [19] is equal to

$$10(2M+1)^2 N_s + 4(2M+1)^3 + \frac{360}{\Delta_\theta}(2M+1)^2 + N_N\frac{2D^2/\lambda - 0.62\sqrt{D^3/\lambda}}{\Delta_r}(2M+1)^2. \tag{38}$$

In the proposed method, four FOC matrices with dimensions $(2M-1) \times (2M-1)$ and one $(2M+1) \times (2M+1)$ FOC matrix are constructed from the received data. It also requires the construction of matrices $\mathbf{C}_A$ and $\mathbf{C}_N$, in which pseudo-inversion operations are computed for them. The EVD is applied on $\mathbf{C}_A$ of size $(2M+1) \times (2M+1)$ and on $\mathbf{C}_N$ of size $(2M-1) \times (2M-1)$. It does not require any search process. Therefore, the number of operations required in the proposed method is equal to

$$36(2M-1)^2 N_s + 9(2M+1)^2 N_s + 2\left((2M+1)^3 + (2M-1)^3\right) + 2M(2M+1)^2 + (2M-1)^3. \tag{39}$$

In general, it can be concluded that in terms of statistics matrices construction, the methods [15] and [8] have the least complexity, and the most one belongs to the method [11]. In terms of eigen decomposition, the proposed method and method [8] have the lowest computations, and method [7] has the highest one. In terms of spectral search, only the proposed method has no processing stage, and other methods (especially for small search steps) require significant processing burden.

4.2. Aperture Loss

The method [7] that is based on MUSIC technique constructs two $(2M+1) \times (2M+1)$ and $(4M+1) \times (4M+1)$ matrices. Given the subspace theory [27], it requires at least one eigenvector of the matrices to span the noise subspace. So method [7] is able to resolve at most $2M$ sources. In method [8] due to the generation of the overlapping subvectors, a 50% array aperture loss occurs, and the maximum number of resolvable sources is equal to M. In method [15], the parameters of NFSs and FFSs are estimated through two distinct processes. Having N_N NFSs, at least $2N_N+1$ sensors are required. The method [15], in total, is able to resolve at most $2M$ sources. The method [11] does not require subspace

decomposition; however, it requires to ensure that there exists a nonzero vector which is orthogonal to the range space by all the virtual steering vectors except one of them. Such a condition only requires to assume $N \leq 2M + 1$, and in other words, method [11] can resolve $2M + 1$ sources. The method [18] can resolve at most $2M$ sources. In method [19], the signal subspace of the reconstructed matrix is divided into two $2M \times N_N$ matrices. Therefore, it can locate $2M - 1$ NFSs or $2M$ mixed sources at most. According to the explanations given in Sections 3.2 and 3.4, about the constitution of $\mathbf{B}_1$ and $\mathbf{D}_N$, it is necessary that the number of sensors simultaneously satisfy the conditions $2M + 1 \geq N_N + 2$ and $2M + 1 > N$ because full column rank of them requires this. Therefore, in the proposed method, the maximum number of resolvable sources is equal to $2M$.

In general, it can be stated that in terms of avoiding aperture loss, the proposed method has much better performance than the method [8] and is comparable with methods [7, 15, 18, 19].

4.3. Parameters Pairing

Since the DOA and the range of NFSs are both computed in parallel from eigenvalues and eigenvectors of $\mathbf{C}_N$, the proposed method does not require any additional steps for pairing, and this operation is performed automatically.

4.4. NFS Localization at the Same Angle with the FFS

When the NFS is located in the same angle with the FFS, none of the methods [7, 8, 11, 18, 19] is able to estimate correctly. Given the structure of matrix $\mathbf{B}$ that contains virtual steering vectors and is merely dependent on sources' DOA, when two sources have the same angle, its rank is lost.

5. SIMULATION RESULTS

In this section, we present and discuss the simulation results to examine the performance of the proposed method in dealing with mixed NFSs and FFSs. For all examples, an 11-elements ($M = 5$) symmetric ULA with element spacing $d = 0.25\lambda$ is assumed. All sources are equi-power, statistically independent, and with narrowband stationary signals. The additive noise is assumed to be a spatial white complex Gaussian random process. Angle and range search steps in different methods are assumed $0.01°$ and 0.05λ, respectively. We compare the estimation accuracy of the proposed method with the methods [15, 18, 19], and also the related Cramer-Rao bound (CRB) [28]. The results are evaluated in the estimated root mean square error (RMSE) derived from the average of N_T independent Monte-Carlo runs. The RMSE is defined as

$$RMSE = \sqrt{\frac{1}{N_T} \sum_{n=1}^{N_T} \left(\hat{\zeta}_n - \zeta\right)^2} \tag{40}$$

where $\hat{\zeta}_n$ is an estimate of the parameter ζ in the nth experiment. Also, in terms of the probability of correct classification of the signals types versus the signal-to-noise ratio (SNR) and snapshot number, we compare the proposed method with other methods. We define the probability of correct classification of the signals types as

$$P_c = \frac{N_c}{N_T} \tag{41}$$

where N_c is the number of successful classifications. If in a run, the regions of all the sources are correctly determined, this means the correct classification in that execution.

Example 1: In the first simulation, we compare the probability of correct classification of the signals types in the proposed method with other methods versus SNR and snapshot number for 500 independent runs. Two NFSs and one FFS are located at ($\theta_1 = -7°$, $r_1 = 2.2\lambda$), ($\theta_2 = 51°$, $r_2 = 4\lambda$) and ($\theta_3 = 22°$, $r_3 = \infty$). Fig. 2 shows comparative results versus SNR and snapshot number. As seen, in the proposed method, for SNRs above $9\,\mathrm{dB}$ (with 1000 snapshots), P_c is equal to 1, whereas this probability is realized in methods [15, 18, 19] for SNRs above 31, 25, and $31\,\mathrm{dB}$, respectively. This indicates the superiority of the proposed method in the correct classification of the signals types. The
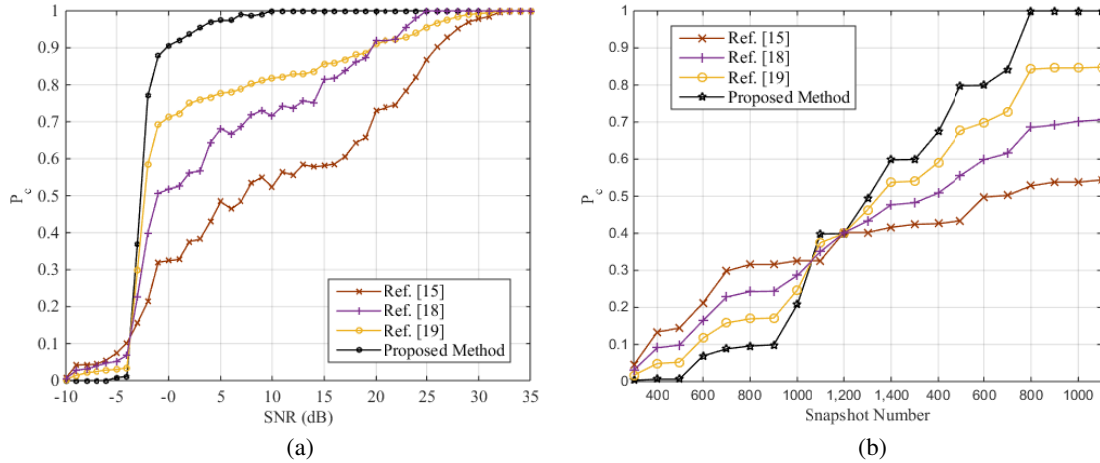
Figure 2. Comparative results of P_c; (a) versus SNR ($N_s = 1000$), (b) versus snapshot number (SNR $= 10$ dB).

reason for the poor classification in method [15] is that it is based on the extraction of noise subspace from the covariance difference matrix. The exact separation of the subspaces of this matrix without the primary knowledge or without the correct estimation of the number of NFSs is a difficult task. However, the proposed method does not need to know the number of NFSs or FFSs, and it performs the classification based on the total information obtained from the vector $\hat{\boldsymbol{\theta}}$ and Eq. (30).

Example 2: In the second test, the estimation accuracy of the proposed method is compared with other methods and also the related CRB versus the SNR and snapshot number. Two NFSs and two FFSs are located at $(\theta_1 = 20°, r_1 = 1.6\lambda)$, $(\theta_2 = 40°, r_2 = 2.9\lambda)$, $(\theta_3 = 0°, r_3 = \infty)$ and $(\theta_4 = -40°, r_4 = \infty)$. The results are obtained from 500 independent trials. In the first case, the number of snapshots is fixed to 750, and SNR varies from -10 to 20 dB. The results of this case are presented in Figs. 3(a) to 3(c). In the second case, the SNR is fixed to 12 dB, and the snapshot number varies from 200 to 1400. The results of this case are presented in Figs. 3(d) to 3(f). As Fig. 3 clearly shows, the diagrams obtained from the proposed method are closer to the related CRBs than the diagrams obtained from the methods [15, 19]. It indicates the superiority of the proposed method in terms of accuracy. The proposed method also has a competitive performance over the method [18]. Due to the use of pure cumulants in the proposed method, with the reduction of the noise effect, it was expected that the accuracy of the proposed method would be better than other methods. The DOA RMSEs for the two NFSs are approximately the same. So according to the analysis of reference [23], in the range estimation, it was expected that the RMSE of the first source would be less than the second one because it is closer to the array. Fig. 3 confirms this.

Example 3: In the third simulation, we compare the computational complexity of the proposed method with the other methods. Here all the assumptions of Example 2 are considered. Fig. 4 shows the computational complexity of the proposed method in comparison with other methods versus the snapshot number. As can be seen, for fewer and moderate snapshots, the proposed method has a much lower total computational complexity than other methods. The elimination of the spectral search stage is the main reason for this excellence. According to the analysis of Section 4.1, it is clear that as the snapshots increase, the term related to the statistics matrices construction becomes the dominant term, and the total complexity follows it. The dominant term in the computational complexity of the method [15] is the spectral search that is independent of the snapshots. That is why the slope of the associated diagram does not change significantly as the snapshot number increases. Since the complexities of methods [18] and [19] are almost the same, their diagrams overlap. It is seen from Fig. 4 that, for 750 snapshots, the computational complexity of the proposed method is lower than the other methods. However, Figs. 2 and 3 show that the proposed method, despite the lower computational complexity, has been able to perform well in classification as well as estimation.

Example 4: In the last simulation, we examine the maximum number of resolvable

sources in the proposed method. Let's consider five NFSs located at $(\theta_1 = -78°, r_1 = 2\lambda)$, $(\theta_2 = -15°, r_2 = 4.4\lambda)$, $(\theta_3 = 6°, r_3 = 2.8\lambda)$, $(\theta_4 = 17°, r_4 = 3.6\lambda)$ and $(\theta_5 = 33°, r_5 = 5.2\lambda)$, and five FFSs located at $(\theta_6 = -51°, r_6 = \infty)$, $(\theta_7 = -40°, r_7 = \infty)$, $(\theta_8 = -30°, r_8 = \infty)$, $(\theta_9 = 50°, r_9 = \infty)$ and $(\theta_{10} = 66°, r_{10} = \infty)$. Snapshot number and SNR are 1024 and 25 dB, respectively. Fig. 5 shows the result of localization for 100 independent experiments. It also indicates the *mean (standard deviation)* derived from DOA and range estimation for each source. Circles, triangles, lines, and pink dashed lines respectively represent the true location of the NFSs, the true DOA of the FFSs, the true location vector of the NFSs, and the true direction vector of the FFSs. The dots and black dashed lines represent the estimated location of the NFSs and the average estimated direction vector of the FFSs, respectively. As shown in Fig. 5, with 11 elements, we are able to detect the corresponding parameters of 10 sources, which confirms the analysis of Section 4.2.
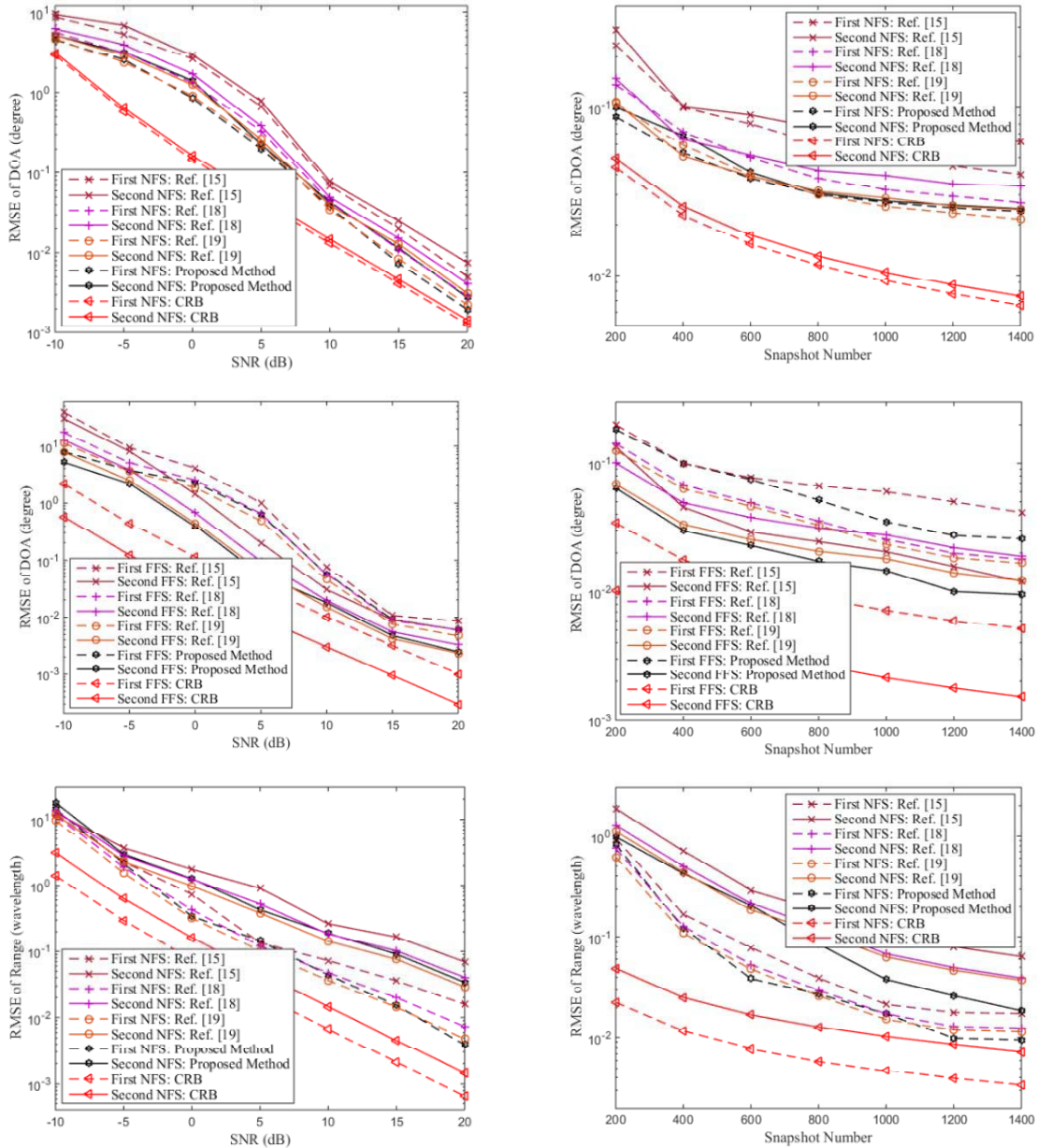
Figure 3.
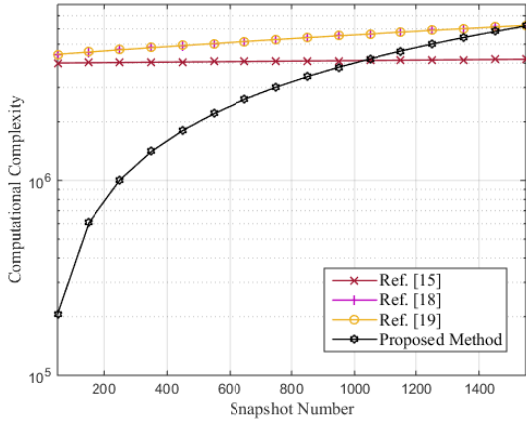
Figure 4. Comparison of the computational complexity of the proposed method with other methods versus snapshot number.
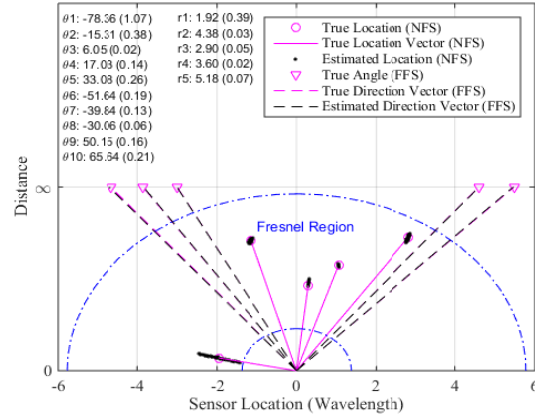
Figure 5. The result of the localization of 10 mixed sources using 11 elements derived from 100 independent runs in the proposed method.

6. CONCLUSIONS

In this paper, a new method is proposed to deal with the simultaneous presence of NFSs and FFSs, using a symmetric ULA. By computing cumulants from the output of array sensors in five special arrangements and efficiently separating the components of NFSs and FFSs by the cumulant differencing, we are able to classify and estimate the parameters of NFSs and FFSs without any spectral search and avoid aperture loss. Since both the DOA and range parameters of the NFSs are estimated from the eigen decomposition of a given matrix, the additional stage for pairing is avoided.

We examine the proposed method in different tests and show that it has a better performance than other methods in the classification and estimation. In the scenario with two NFSs and two FFSs, for SNR 15 dB and with 750 snapshots, the maximum RMSEs of DOA and range are obtained $0.009°$ and 0.08λ in the proposed method, whereas for methods [15, 18, 19] the corresponding values are obtained $0.03°$, $0.01°$, $0.01°$ and 0.17λ, 0.1λ, 0.08λ, respectively. This superiority has been achieved while the proposed method has less computational complexity. We also show that for fewer and moderate snapshots, the proposed algorithm has much less computational complexity than other methods due to the elimination of heavy search steps. In another scenario, with 1000 snapshots, for SNRs above 9 dB, a 100% correct classification of all sources is obtained, whereas this probability was achieved for SNRs above 31, 25, and 31 dB in methods [15, 18, 19], respectively.

To put the proposed method into further applications, future work will be concentrated on the development of the proposed method for more specific scenarios such as the presence of correlated signals and the use of the exact model of the NF.

APPENDIX A. DERIVATION AND ESTIMATION OF (11)

Here, the details of the derivation of the second equation of Eq. (11) are given. Four other equations can be derived in the same way. We commence from Eq. (10)

$$
\begin{aligned}
c_{4x,\,2}\left(u,\,v\right) \; = \; & Cum\left\{x_u^*\left(k\right),\,x_{u+1}\left(k\right),\,x_{v+1}^*\left(k\right),\,x_v\left(k\right)\right\} = E\left\{x_u^*\left(k\right)x_{u+1}\left(k\right)x_{v+1}^*\left(k\right)x_v\left(k\right)\right\} \\
& -E\left\{x_u^*\left(k\right)x_{u+1}\left(k\right)\right\}E\left\{x_{v+1}^*\left(k\right)x_v\left(k\right)\right\} - E\left\{x_u^*\left(k\right)x_{v+1}^*\left(k\right)\right\}E\left\{x_{u+1}\left(k\right)x_v\left(k\right)\right\} \\
& -E\left\{x_u^*\left(k\right)x_v\left(k\right)\right\}E\left\{x_{u+1}\left(k\right)x_{v+1}^*\left(k\right)\right\}.
\end{aligned}
\tag{A1}
$$

The first mathematical expectation in Eq. (A1) can be written as Eq. (A2). In the same way, three other mathematical expectations can be computed. Because all signals are uncorrelated to each other and to the noise (assumptions 2 and 3), we can rewrite Eq. (A2) as Eq. (A3). Since the noise is Gaussian

(assumption 3), the terms concerning noise are neutralized by each other. Finally, with respect to being stationary signals (assumption 2), Eq. (11) is obtained.

$$
E\left\{x_u^*(k)x_{u+1}(k)x_{v+1}^*(k)x_v(k)\right\} = E\left\{\left[\sum_{i=1}^{N_N} s_i^*(k) e^{-j(\gamma_i u + \phi_i u^2)} + \sum_{i=N_N+1}^{N} s_i^*(k) e^{-j\gamma_i u} + n_u^*(k)\right]\right.
$$

$$
\times \left[\sum_{l=1}^{N_N} s_l(k) e^{j(\gamma_l(u+1) + \phi_l(u+1)^2)} + \sum_{l=N_N+1}^{N} s_l(k) e^{j\gamma_l(u+1)} + n_{u+1}(k)\right]
$$

$$
\left[\sum_{m=1}^{N_N} s_m^*(k) e^{-j(\gamma_m(v+1) + \phi_m(v+1)^2)} + \sum_{m=N_N}^{N} s_m^*(k) e^{-j\gamma_m(v+1)} + n_{v+1}^*(k)\right]
$$

$$
\left.\times \left[\sum_{o=1}^{N_N} s_o(k) e^{j(\gamma_o v + \phi_o v^2)} + \sum_{o=N_N+1}^{N} s_o(k) e^{j\gamma_o v} + n_v(k)\right]\right\} \tag{A2}
$$

$$
c_{4x,2}(u,v) = \sum_{i=1}^{N_N} E\left\{s_i^*(k) s_i(k) s_i^*(k) s_i(k)\right\} e^{j2\phi_i(u-v)} + \sum_{i=N_N+1}^{N} E\left\{s_i^*(k) s_i(k) s_i^*(k) s_i(k)\right\}
$$

$$
- \left[\sum_{i=1}^{N_N} E\left\{s_i^*(k) s_i(k)\right\}\right]\left[\sum_{i=1}^{N_N} E\left\{s_i^*(k) s_i(k)\right\}\right] e^{j2\phi_i(u-v)}
$$

$$
- \left[\sum_{i=N_N+1}^{N} E\left\{s_i^*(k) s_i(k)\right\}\right]\left[\sum_{i=N_N+1}^{N} E\left\{s_i^*(k) s_i(k)\right\}\right]
$$

$$
- \left[\sum_{i=1}^{N_N} E\left\{s_i^*(k) s_i^*(k)\right\}\right]\left[\sum_{i=1}^{N_N} E\left\{s_i(k) s_i(k)\right\}\right] e^{j2\phi_i(u-v)}
$$

$$
- \left[\sum_{i=N_N+1}^{N} E\left\{s_i^*(k) s_i^*(k)\right\}\right]\left[\sum_{i=N_N+1}^{N} E\left\{s_i(k) s_i(k)\right\}\right]
$$

$$
- \left[\sum_{i=1}^{N_N} E\left\{s_i^*(k) s_i(k)\right\}\right]\left[\sum_{i=1}^{N_N} E\left\{s_i(k) s_i^*(k)\right\}\right] e^{j2\phi_i(u-v)}
$$

$$
- \left[\sum_{i=N_N+1}^{N} E\left\{s_i^*(k) s_i(k)\right\}\right]\left[\sum_{i=N_N+1}^{N} E\left\{s_i(k) s_i^*(k)\right\}\right]
$$

$$
+ E\left\{n_u^*(k) n_{u+1}(k) n_{v+1}^*(k) n_v(k)\right\} - E\left\{n_u^*(k) n_{u+1}(k)\right\} E\left\{n_{v+1}^*(k) n_v(k)\right\}
$$

$$
- E\left\{n_u^*(k) n_{v+1}^*(k)\right\} E\left\{n_{u+1}(t) n_v(t)\right\} - E\left\{n_u^*(k) n_v(k)\right\} E\left\{n_{u+1}(k) n_{v+1}^*(k)\right\} \tag{A3}
$$

$c_{4x,2}(u,v)$ can be estimated from the following equation:

$$
\hat{c}_{4x,2}(u,v) = \frac{1}{N_s} \sum_{k=1}^{N_s} \bar{x}_u^*(k) \bar{x}_{u+1}(k) \bar{x}_{v+1}^*(k) \bar{x}_v(k) - \frac{1}{N_s^2} \sum_{k=1}^{N_s} \bar{x}_u^*(k) \bar{x}_{u+1}(k) \sum_{k=1}^{N_s} \bar{x}_{v+1}^*(k) \bar{x}_v(k)
$$

$$
- \frac{1}{N_s^2} \sum_{k=1}^{N_s} \bar{x}_u^*(k) \bar{x}_{v+1}^*(k) \sum_{k=1}^{N_s} \bar{x}_{u+1}(k) \bar{x}_v(k) - \frac{1}{N_s^2} \sum_{k=1}^{N_s} \bar{x}_u^*(k) \bar{x}_v(k) \sum_{k=1}^{N_s} \bar{x}_{u+1}(k) \bar{x}_{v+1}^*(k) \tag{A4}
$$

where $\bar{x}_i(t) = x_i(t) - E_i$, and E_i is obtained from averaging the data received from the ith sensor.

APPENDIX B. THE PROOF OF BEING TOEPLITZ OF THE MATRICES OF EQ. (22)

Here we prove that $\mathbf{C}_{N1}$ is a Toeplitz matrix. It suffices to show that $\mathbf{C}_{N1}(\tilde{u}+1,\tilde{v}+1) = \mathbf{C}_{N1}(\tilde{u},\tilde{v})$. According to Eq. (13)

$$\mathbf{C}_{N1}(\tilde{u}+1,\tilde{v}+1) = \sum_{i=1}^{N_N} c_{s_i} e^{j2\phi_i(\tilde{u}+1-(\tilde{v}+1))} = \sum_{i=1}^{N_N} c_{s_i} e^{j2\phi_i(\tilde{u}-\tilde{v})} \tag{B1}$$

which is equal to $\mathbf{C}_{N1}(\tilde{u},\tilde{v})$. In a similar manner, it is easy to prove five other five matrices being Toeplitz.

REFERENCES

1. Tuncer, T. E. and B. Friedlander, *Classical and Modern Direction-of-Arrival Estimation*, Academic Press, 2009.
2. Huang, Y.-D. and M. Barkat, "Near-field multiple source localization by passive sensor array," *IEEE Transactions on Antennas and Propagation*, Vol. 39, 968–975, 1991.
3. Chen, J.-F., X.-L. Zhu, and X.-D. Zhang, "A new algorithm for joint range-DOA-frequency estimation of near-field sources," *EURASIP Journal on Advances in Signal Processing*, Vol. 2004, 105173, 2004.
4. Goh, S. T., S. A. R. Zekavat, and K. Pahlavan, "DOA-based endoscopy capsule localization and orientation estimation via unscented Kalman filter," *IEEE Sensors Journal*, Vol. 14, 3819–3829, 2014.
5. Tichavsky, P., K. T. Wong, and M. D. Zoltowski, "Near-field/far-field azimuth and elevation angle estimation using a single vector hydrophone," *IEEE Transactions on Signal Processing*, Vol. 49, 2498–2510, 2001.
6. Jiang, J.-J. F.-J. Duan, J. Chen, Y.-C. Li, and X.-N. Hua, "Mixed near-field and far-field sources localization using the uniform linear sensor array," *IEEE Sensors Journal*, Vol. 13, 3136–3143, 2013.
7. Liang, J. and D. Liu, "Passive localization of mixed near-field and far-field sources using two-stage MUSIC algorithm," *IEEE Transactions on Signal Processing*, Vol. 58, 108–120, 2010.
8. He, J., M. Swamy, and M. O. Ahmad, "Efficient application of MUSIC algorithm under the coexistence of far-field and near-field sources," *IEEE Transactions on Signal Processing*, Vol. 60, 2066–2070, 2012.
9. Liu, G., X. Sun, Y. Liu, and Y. Qin, "Low-complexity estimation of signal parameters via rotational invariance techniques algorithm for mixed far-field and near-field cyclostationary sources localisation," *IET Signal Processing*, Vol. 7, 382–388, 2013.
10. Wang, B., Y. Zhao, and J. Liu, "Mixed-order MUSIC algorithm for localization of far-field and near-field sources," *IEEE Signal Processing Letters*, Vol. 20, 311–314, 2013.
11. Xie, J., H. Tao, X. Rao, and J. Su, "Passive localization of mixed far-field and near-field sources without estimating the number of sources," *Sensors*, Vol. 15, 3834–3853, 2015.
12. Gao, F. and A. B. Gershman, "A generalized ESPRIT approach to direction-of-arrival estimation," *IEEE Signal Processing Letters*, Vol. 12, 254–257, 2005.
13. Liu, G. and X. Sun, "Efficient method of passive localization for mixed far-field and near-field sources," *IEEE Antennas and Wireless Propagation Letters*, Vol. 12, 902–905, 2013.
14. Liu, G. and X. Sun, "Spatial differencing method for mixed far-field and near-field sources localization," *IEEE Signal Processing Letters*, Vol. 21, 1331–1335, 2014.
15. Liu, G. and X. Sun, "Two-stage matrix differencing algorithm for mixed far-field and near-field sources classification and localization," *IEEE Sensors Journal*, Vol. 14, 1957–1965, 2014.
16. Zhi, W. and M. Y.-W. Chia, "Near-field source localization via symmetric subarrays," *2007 IEEE International Conference on Acoustics, Speech and Signal Processing, ICASSP'07*, II-1121–II-1124, 2007.

17. Xie, J., L. Wang, and J. Su, "Parameters estimation of mixed far-field and near-field sources via second order statistics," *2017 International Applied Computational Electromagnetics Society Symposium (ACES)*, 1–2, 2017.

18. Zheng, Z., J. Sun, W.-Q. Wang, and H. Yang, "Classification and localization of mixed near-field and far-field sources using mixed-order statistics," *Signal Processing*, Vol. 143, 134–139, 2018.

19. Zheng, Z., M. Fu, D. Jiang, W.-Q. Wang, and S. Zhang, "Localization of mixed far-field and near-field sources via cumulant matrix reconstruction," *IEEE Sensors Journal*, Vol. 18, 7671–7680, 2018.

20. Liang, J., "Joint azimuth and elevation direction finding using cumulant," *IEEE Sensors Journal*, Vol. 9, 390–398, 2009.

21. Begriche, Y., M. Thameri, and K. Abed-Meraim, "Exact Cramer Rao bound for near field source localization," *2012 11th International Conference on Information Science, Signal Processing and their Applications (ISSPA)*, 718–721, 2012.

22. Grosicki, E., K. Abed-Meraim, and Y. Hua, "A weighted linear prediction method for near-field source localization," *IEEE Transactions on Signal Processing*, Vol. 53, 3651–3660, 2005.

23. Yuen, N. and B. Friedlander, "Performance analysis of higher order ESPRIT for localization of near-field sources," *IEEE transactions on Signal Processing*, Vol. 46, 709–719, 1998.

24. Duofang, C., C. Baixiao, and Q. Guodong, "Angle estimation using ESPRIT in MIMO radar," *Electronics Letters*, Vol. 44, 770–771, 2008.

25. Liu, F., J. Wang, C. Sun, and R. Du, "Spatial differencing method for DOA estimation under the coexistence of both uncorrelated and coherent signals," *IEEE Transactions on Antennas and Propagation*, Vol. 60, 2052–2062, 2012.

26. Golub, G. H. and C. F. Van Loan, *Matrix Computations*, Vol. 3, JHU Press, 2012.

27. Paulraj, A., *Subspace Methods for Direction of Arrival Estimation*, Handbook of Statistics, 10 Eds. Bose NK and Rao, CR, North-Holland, ed., 1993.

28. Molaei, A. M., B. Zakeri, and S. M. H. Andargoli, "Closed-form expression of stochastic crb for mixed near-field and far-field sources in multipath propagation environments," *IEEE Communications Letters*, Vol. 23, 640–643, 2019.